The fall and rise of metamorphic zircon

Revision 1

Matthew J. Kohn[1] (corresponding author), Stacey L. Corrie[1], and Christopher Markley[1]

[1]*Department of Geosciences, Boise State University, Boise, ID 83725; mattkohn@boisestate.edu*

phone: 208-426-2757; fax: 208-426-4061

Abstract

Zircon geochronology and geochemistry are increasingly important for understanding metamorphic processes, particularly at extreme conditions, but drivers of zircon dissolution and regrowth are poorly understood. Here, we model Zr mass balance to identify P-T regions where zircon should dissolve or grow. Zirconium contents of major metamorphic minerals were assessed from published data and new measurements, and models were constructed of mineralogical development and zircon abundance for hydrous MORB and metapelitic compositions along representative P-T paths. Excluding zircon, the minerals rutile, garnet and hornblende strongly influence Zr mass balance in metabasites, accounting for as much as 40% of the whole-rock Zr budget. Clinopyroxene and garnet contain more Zr than plagioclase, so breakdown of plagioclase at the amphibolite to eclogite facies transition, should cause zircon to dissolve slightly, rather than grow. Growth of UHP zircon is predicted over a restricted region, and most zircon grows subsequently at much lower pressure. In metapelites, zircon is predicted to undergo only minor changes to modal abundance in solid state assemblages. Partial melting, however, drives massive zircon dissolution, whereas melt crystallization regrows zircon. From a mass balance perspective, zircon growth cannot be attributed *a priori* to the prograde amphibolite-eclogite transition, to UHP metamorphism, or to partial melting. Instead, zircon should grow mainly during late-stage exhumation and cooling, particularly during oxide transitions from rutile to ilmenite and melt crystallization. As predicted, most zircons from HP/UHP eclogites of the Western Gneiss Region and Papua New Guinea substantially postdate eclogite formation and maximum pressures.

Keywords: Trace elements and REE: Zr, zircon; Metamorphic petrology: UHP, metabasite; Geochronology: zircon

Introduction

Zircon has long served an important chronologic role, and it is now used nearly ubiquitously to investigate metamorphic rocks that formed under extreme conditions – ultra-high pressure (UHP), ultra-high temperature (UHT), or both. One common assumption in UHP studies is that zircon grows at peak pressures, so metamorphic zircons directly date UHP metamorphism. While perhaps true, no rigorous theoretical justification of this assumption has been offered. An alternative implicit assumption in other studies – that zircon can grow essentially at any point along a pressure-temperature (P-T) path – appears unlikely to us for two reasons. First, zircon resists deformation, as witnessed by its retention of relict cores, so it is unlikely to accumulate defects and recrystallize. Second, minerals other than zircon have varying affinities (saturation contents) for Zr. Mass balance in reacting rocks therefore demands that as mineral assemblages and abundances change along a P-T path, this non-zircon portion of the rock will either take up or release Zr. Thus, mineral assemblage shifts may produce zircon along some portions of a P-T path but should consume zircon along others.

But, what systematics occur in such reactive systems? Is the amount of Zr taken up by non-zircon phases trivial, or can certain assemblages at specific conditions accommodate a significant portion of the total Zr? If the latter, are certain P-T trajectories or regions of P-T space, e.g. peak UHP conditions, more conducive to zircon production so are more likely to be represented by zircon ages? In the context of these questions, we first evaluated Zr saturation contents of common metamorphic minerals in equilibrium with zircon. This allowed us to evaluate what minerals other than zircon affect whole rock Zr mass balance, for example finding that plagioclase, sheet silicates, lawsonite, and low-T amphiboles have generally low Zr contents (<1 ppm; 1 ppm = 1 μg/g) whereas rutile, garnet, hornblende, epidote, clinopyroxene and titanite dominate the non-zircon mineral portion of the Zr budget (>>1 ppm; Bea et al., 2006). Second we modeled hydrous MORB and metapelite compositions and tracked changes in mineral modes and Zr contents along three hypothetical P-T paths: (1) relatively low-T, UHP similar to the Alps (“Alpine-type”; e.g. Chopin et al., 1991; Schertl et al., 1991), (2) high-T, high-P similar to the Western Gneiss region (“WGR-type”;

e.g., Carswell et al., 2003a), and (3) moderate-T, moderate-P as predicted theoretically for continental collisions ("CC-type"; e.g. England and Thompson, 1984). These models allow us to generalize about what portions of a P-T path or regions of P-T space are likely to induce zircon growth, and help frame studies of metamorphic zircon chronology. We particularly emphasize implications for studies of UHP or near-UHP rocks. Our work parallels pioneering studies of zircon and monazite growth in lower P felsic compositions (Kelsey et al., 2008; Kelsey and Powell, 2011), but addresses a different region of P-T space as well as different bulk compositions.

Methods

Zirconium contents of common metamorphic minerals were compiled from the literature (Table 1) and from new measurements at Boise State University. See the Supplemental data file for full data, data sources, methods and assumptions regarding saturation contents. We found no obvious T-dependence for the Zr content in most minerals except garnet and hornblende, which consequently must be modeled (Fig. 1; Kelsey and Powell, 2011). One possible expression for equilibrium between zircon and the Zr component in garnet (Tomkins, 2006) is:

$$Fe_3Zr_2Al_2SiO_{12} + 4SiO_2 = Fe_3Al_2Si_3O_{12} + 2ZrSiO_4. \quad \text{Eq. 1}$$

Assuming (a) saturation with nearly pure quartz and zircon (true for most rocks, including metabasalts of MORB composition), (b) Henry's law behavior for Zr mixing (expected for trace elements), and (c) broadly similar garnet compositions (so that the mole fraction of the Zr component corresponds to a similar weight fraction of Zr – also true in most rocks), thermodynamic expressions predict a linear relationship between the logarithm of Zr content in garnet as measured in ppm and the reciprocal of absolute T (Tomkins, 2006). A similar equilibrium and corresponding expression are possible for hornblende. Consequently, we regressed ln(Zr) of garnet and hornblende vs. P and 1/T, where Zr is measured in ppm and T is in kelvins, using an unweighted linear least squares method. Temperatures and pressures were taken from original publications or are otherwise tabulated in the supplemental file, and are primarily based on major element thermobarometry either in each rock or in the region. The coefficient for P was indistinguishable from zero, so this term was dropped from

models. Hornblende and garnet show nearly identical correlation between ln(Zr) and 1/T (Fig. 1), so our preferred expression combines them into a single overall regression, which we use to model compositions for both minerals. Note that if garnet and hornblende compositions reported in the literature reflect retention of lower-T Zr contents to higher T, only the higher concentrations should be regressed to determine T-dependencies. If so, our theoretical models could underestimate the impact of garnet and hornblende on Zr mass balance, and overestimate the amount of zircon in a rock. Such a change does not significantly affect our conclusions.

We constructed bulk composition-specific mineral assemblage diagrams (pseudosections) for two different rocks. For mafic pseudosections, we assumed an average global MORB composition (Arevalo and McDonough, 2010) with a Zr content of 100 ppm, correcting Ca content for apatite (based on P_2O_5). We calculated stable assemblages using TheriakDomino (de Capitani and Petrakakis, 2010), which allows automated calculations of pseudosections (using Domino) and mineral abundances and compositions at specified P-T conditions (using Theriak). Two MORB models were constructed corresponding to the thermdynamic databases of Holland and Powell (1998) and Berman (1988; also Berman and Aranovich, 1996). Besides differences in endmember thermochemical properties, these approaches use complex vs. simple mixing models for amphiboles and other multi-site silicates and generally overpredict vs. underpredict blueschist stability (glaucophane abundance). The Holland and Powell model also overpredicts stability of coexisting amphibole assemblages. Overall, however, the models bracket any likely range of mineral assemblages, and fortunately make nearly identical predictions with respect to Zr modeling. Although we do not recommend using the models to predict P-T paths from major element chemistry or specific mineral assemblages, they are sufficiently accurate for Zr mass balance to identify first-order impacts on zircon abundance.

For the metapelite pseudosection, we followed Kelsey et al. (2008) and Kelsey and Powell (2011) in using the Holland and Powell (1998) database but assumed a representative bulk composition from Spear et al. (1990) modified by adding 1 wt% TiO_2 and 200 ppm Zr (Taylor and McLennan, 1985). In comparison to Kelsey et al. (2008) and Kelsey and Powell (2011), our model

assumes lower Ti and H_2O, which reduces the predicted amount of rutile and melt, and consequently minimizes the amount of dissolved zircon. The Supplemental file presents the pseudosections (Fig. S1, S2) and provides additional discussion of thermodynamic solution models.

Results

For the MORB compositions, the two pseudosection models imply somewhat different mineral stability fields (Figs. 2, S1). For example, garnet and rutile are more stable in the Holland and Powell model than in the Berman model. The Holland and Powell model also predicts large regions in which multiple amphiboles are stable together such as glaucophane + actinolite and hornblende + actinolite (Fig. S1), whereas equilibrium natural occurrences of these assemblages are extremely rare. Nonetheless, both models imply that exhumation and cooling destabilize rutile and stabilize plagioclase. Because rutile contains high Zr contents at high T, whereas plagioclase does not, Zr should become available for new zircon growth. That is, zircon should grow during exhumation and cooling (red arrows in Figs. 2-3). The Alpine-path predicts zircon growth over a larger range of pressure because cooling occurs in closer proximity to peak P-T conditions compared to the WGR- and CC-paths. Because the Zr content of rutile increases with increasing T and decreasing P (Fig. 3; Zack et al., 2004; Watson et al., 2006), both heating and isothermal exhumation tend to consume zircon to provide Zr to rutile (Figs. 2-3). The WGR- and CC-paths show extensive heating after reaching peak pressure, and more nearly isothermal exhumation initially. These factors reduce the range of pressures over which zircon is expected to grow.

For the metapelite (Figs. 3B, S2), solid-state and dehydration reactions also generally drive dissolution of zircon during prograde metamorphism, but by much smaller proportional amounts than in metabasites. Although Ti contents and modeled rutile modes are similar, metabasites contain far more amphibole and garnet, which take up more Zr than most other minerals, and metapelites contain twice the Zr content so the relative impact is smaller. Most importantly, our model confirms conclusions of Kelsey et al. (2008) and Kelsey and Powell (2011) that melting reactions in felsic rocks dominate zircon consumption and production. Massive dissolution of zircon occurs as rocks

cross melting reactions (Fig. 3B; Kelsey et al., 2008; Kelsey and Powell, 2011), because melts take up so much Zr (Watson and Harrison, 1983; Boehnke et al., 2013). As T increases and P decreases, additional zircon dissolves through increased melt fraction and changes to melt chemistry (Fig. 3, WGR path). This Zr is held in melts until cooling drives crystallization, whereupon zircon regrows.

Overall, Zr mass balance (Figs. 3-5) shows that matrix minerals and melts take up progressively more Zr during prograde metamorphism and the initial stages of exhumation until the maximum temperature is reached, rutile breaks down to form ilmenite or titanite, or melts begin to crystallize. In all models, the amount of dissolved zircon in the WGR-path substantially exceeds that of the CC- and Alpine-paths. At the high-T low-P conditions reached during exhumation on the WGR-path, rutile, garnet and hornblende (in metabasites) take up the most Zr, and melts (in metapelites) are most abundant and their chemistry dissolves more zircon. In metapelites, differences in the amount of melt produced along each path (Alpine = none; CC = small; WGR = large) strongly influence the predicted amount of zircon dissolved (Figs. 3B, 5). In metabasites, small reversals in zircon growth during exhumation are possible, for example as the rock re-enters rutile-stability in the Berman model of the WGR path, or as amphiboles transform from low-Zr glaucophane to high-Zr hornblende in the Holland and Powell model of the Alpine path.

Discussion

How does zircon grow?

Our models generally imply that many metamorphic assemblages, especially those containing rutile, garnet, hornblende and melt, take up progressively more Zr during prograde metamorphism and initial exhumation. The effect of melting on zircon abundance is especially striking (Figs. 3B, 5; Kelsey et al., 2008; Kelsey and Powell, 2011). Presuming that zircon is the primary host of Zr in a rock, uptake of Zr in minerals and melts requires that the mode of zircon decreases during prograde metamorphism, i.e. zircon should dissolve. The same processes operating in reverse (decreasing T, destabilization of rutile, melt crystallization, etc.) return Zr to the matrix during exhumation and cooling. If zircon remains the primary host of Zr, zircon grows at this

metamorphic stage.

Seminal UHT studies demonstrate that zircon can grow at the expense of high-Zr, occasionally relict igneous phases, including high-T garnet, hornblende, pyroxene, and oxides (Fraser et al., 1997; Degeling et al., 2001; Bingen et al., 2001). These previous studies differ from our results, however, because the precursor phases formed at such unusually high T that simple cooling and decreasing Zr solubility can drive zircon growth as Zr diffuses out of the host phase and reacts with silicic matrix minerals. Although our work firmly supports the conclusions of these previous studies, we further show that mineral transitions over a range of metamorphic grades, not just UHT, could play an important role in the growth of metamorphic zircon. The conclusion that cooling during exhumation can drive zircon growth over a large region of P-T space (Alpine-path; Fig. 2) parallels studies of Kokchetav UHP rocks (Hermann et al., 2001), which exhibit a qualitatively similar path, albeit reaching much higher pressures.

Major mineral transitions do not always impact Zr mass balance significantly. For example, the prograde breakdown of plagioclase and glaucophane to form omphacite and garnet (transition to eclogite facies) takes up less than 0.5% of whole-rock Zr, typically only ~0.2%. Instead absolute T and the stability and abundance of Ti-phases and melts play a much larger role. Indeed, the largest abrupt changes to Zr distributions reflect the formation and demise of rutile and melts (Figs. 2-5; Kelsey et al., 2008; Kelsey and Powell, 2011), coupled with a strong T-dependence to the Zr content of melt, rutile, hornblende and garnet (Fig. 1; Watson and Harrison, 1983; Zack et al., 2004; Watson et al., 2006; Kelsey and Powell, 2011; Boehnke et al., 2013; Figs. 1, 3). Among Ti-rich minerals, ilmenite and titanite also take up Zr, but solubility in rutile is so much higher that transitions from rutile to ilmenite and titanite should catalyze zircon growth. For example, maximum calculated Zr contents for rutile vs. titanite in our models are ~1500 vs. ~250 ppm, and ilmenite typically contains less than 10 ppm Zr. The basic principle that Zr is preferentially incorporated into melt, rutile, garnet, and hornblende with increasing T and decreasing P helps frame interpretation of data from UHP terranes discussed below.

Although our models imply zircon dissolution during prograde metamorphism and early

stages of uplift, the amount dissolved should rarely, if ever, approach 100% (Figs. 3-5). Thus, if new zircon preferentially grows on existing crystals, metamorphic zircons should inevitably retain relict cores. Cathodoluminescence (CL) images of metamorphic zircons nearly always show different CL brightness or zoning patterns in cores vs. rims, and the ages of cores commonly correspond with either the protolith age directly (if the rock is metaigneous), or older source regions (if zircons are detrital). In this respect, our models explain in theoretical context not only why relict cores are so common, but also the historic shift from whole-grain analysis (usually by TIMS) to microanalysis that avoids mixing relict cores and metamorphic rims.

Our models also illustrate that zircon growth rates should vary along a specific P-T path or among different bulk compositions. For example, rapid zircon growth could occur as partial melts crystallize over a much smaller range of pressures or temperatures (or both) compared to other stages along the P-T path or in other bulk composition rocks experiencing the same path. Consequently, age uniformity vs. gradients may not require rapid vs. slow cooling, but rather reflect the expected variations in zircon growth rates as different reactions (e.g. melt crystallization, formation of ilmenite, etc.) or the temperature-dependence of Zr solubilities in minerals (e.g., Zr-in-rutile) differentially impact zircon modes.

Other considerations

Titanium uptake in other silicates. Our models do not account for Ti uptake in other minerals, especially biotite and hornblende. For example, the Ti content of biotite increases strongly with temperature (Henry et al., 2005), and exchange equilibria involving Ti components in micas and hornblende depend strongly on T but not significantly on P (Chambers and Kohn, 2012). These considerations imply that up to the maximum T, biotite and hornblende will take up Ti and reduce the abundance of rutile. Because rutile contains far more Zr than silicates (other than zircon), the amount of zircon dissolved should be lower than we calculated. Although this process can become important at low P (e.g. CC-path), most zircon dissolution in mafic eclogites is predicted to occur where biotite and hornblende are not stable, and in metapelites melting takes over at lower P as the

dominant control on Zr mass balance. For these reasons, we view Ti contents of amphiboles and micas as of secondary importance.

Melting. Melting reactions strongly affect zircon consumption and growth (Figs. 3B, 5; Kelsey et al., 2008; Kelsey and Powell, 2011): melting initially consumes zircon because the melt has high Zr content, whereas melt crystallization produces zircon. For metapelitic rocks, the effect is massive, and more than 50% of zircon can dissolve. For mafic rocks, our model paths do enter the wet-melting region, but the amount of melt will be small, and, unlike in metapelites, no major dehydration-melting reactions are encountered. Thus, melting is crucial for understanding zircon behavior in felsic rocks (Figs 3B, 5; Kelsey et al., 2008; Kelsey and Powell, 2011), but may be insignificant for mafic rocks.

In detail, the exact P-T trajectory for felsic migmatites defines whether zircon grows or dissolves after initial melting and during uplift. At high-T, low-P condition, modal isopleths have slopes similar to Zr-in-rutile (Kelsey et al., 2008; Fig. 3B). If uplift occurs nearly isothermally (WGR-type), zircon will dissolve, and it will regrow only during late-stage exhumation and cooling. This result essentially parallels predictions of our melt-absent models (Fig. 3A). In contrast, if uplift occurs with cooling, decreasing solubility of zircon with decreasing T might overcome small increases in melt fraction, and zircon could crystallize (Hermann et al., 2001).

Comparison to studies of UHP rocks.

Western Gneiss Region. Numerous chronologic data from HP/UHP rocks of the Western Gneiss Region permit comparison of the relative timing of mineral formation. Titanite is not stable above P~15 kbar for most bulk compositions (Spencer et al., 2013; Figs. 2, S1, S2), so a key thermal-chronologic dataset from titanite (Spencer et al., 2013) allows construction of the post-HP/UHP T-t curve (Fig. 6). Individual ages range from ~385 to ~405 Ma, implying post-eclogite-facies conditions by c. 405 Ma. By comparing titanite and zircon crystallization ages, we can identify zircon that must have formed at P<15 kbar. We assume that titanite ages are not diffusionally biased

because age systematics and the preservation of relict titanite cores in high-T rocks imply retention of primary U-Pb ages up to at least 775 °C (Kohn and Corrie, 2011; Gao et al., 2012; Spencer et al., 2013). Experimental measurements, however, do imply relatively fast diffusion of Pb in titanite and a low closure temperature (<650 °C; see Cherniak, 2010) – a discrepancy compared to natural data that is as yet unexplained. Any diffusional resetting of titanite would imply that the measured ages are younger than titanite crystallization, so the time at which rocks exhumed to 15 kbar is earlier than we assume, i.e. ≥405 Ma. Ignoring this potential bias makes our interpretations chronologically conservative.

Zircon ages range between ~425 and ~390 Ma, and most (75%) overlap with titanite ages (Fig. 6). Because titanite formed below 15 kbar, so too must have the majority of zircon, as predicted in Figs. 2-5 for mafic and felsic compositions. Many of these zircon data are from relatively felsic compositions, and crystallization probably occurred from melts. Nonetheless, modeling of these compositions indicates that rutile was stable at HP/UHP conditions (Spencer et al., 2013). Thus, the main principle espoused here appears relevant – zircon growth must have been facilitated by the high-temperature transition from rutile to titanite during exhumation and by the crystallization of *in situ* melts during cooling. Thus most zircon grew far from UHP conditions.

In contrast to our proposal, many zircons from the Western Gneiss Region are inferred to have formed during HP or UHP metamorphism. In part this interpretation is based on trace element patterns indicating formation in the presence of garnet (“flat HREE”) and supposed absence of plagioclase (no Eu-anomaly; Gordon et al., 2013), but an equant crystal morphology is another primary criterion (e.g. Krogh et al., 2011). Although detailed discussion of these issues is beyond the scope of the present study (see Kohn and Spear, 2015), we note the following: (1) Garnet stability occurs relatively early in the metamorphic cycle (Figs. 2, S1, S2), and garnet is commonly reported as a matrix mineral. So, even ignoring questions of whether trace elements equilibrate effectively during metamorphism (e.g., Chernoff and Carlson, 1999; Kohn, 2004; Gordon et al., 2012; Zirakparvar et al., 2014), zircon could coexist with garnet any time from pre-eclogite conditions to the latest stages of uplift and cooling. That is, zircon could form below 15 kbar, as our models predict,

and still encode flat HREE patterns. (2) Plagioclase takes up Eu^{2+}, whereas zircon takes up Eu^{3+}, so the demise of plagioclase and release of Eu^{2+} during the amphibolite-eclogite transition does not necessarily exert any control over Eu($^{3+}$)-anomalies in zircon. (3) Even if zircon morphology does discriminate metamorphic grains, the metamorphic cycle encompasses a wide range of P-T conditions, so this fact alone is not very diagnostic petrogenetically.

Last, some might argue that Sm-Nd and Lu-Hf ages from HP and UHP garnets provide *prima facie* evidence for HP/UHP metamorphism between at least 395 and 420 Ma, which also overlaps most zircon ages (Fig. 6). However, no dated garnets were characterized for trace element zoning, especially the distributions of Sm, Nd and Lu. Relatively fast diffusion of Sm and Nd predicts diffusional resetting with closure temperatures in the range 700-775 °C (depending on cooling rate; Burton et al., 1995; Ganguly et al., 1998) for many ~1 mm-scale garnet crystals that have been dated (Kylander-Clark et al., 2007). Such low closure temperatures overlap Zr-in-titanite T's, indicating that younger Sm-Nd ages cannot reflect UHP conditions. Possible bias to the Lu-Hf system depends on competing effects of dissolution and diffusion. Lutetium diffuses faster than Hf in garnet (Bloch, 2013) and largely controls diffusive resetting (Kohn, 2009). Outward-diffusion of Lu from garnet cores and uptake on garnet rims should rotate isochrons to steeper slopes and cause spuriously old ages (Kohn, 2009; Bloch, 2013). Thus, the fact that Lu-Hf ages are older and show less variation than Sm-Nd ages does not necessitate more accurate dating of peak UHP metamorphism.

In sum, until garnet ages are united with more comprehensive geochemical and petrologic analysis, titanite ages provide the more compelling lower limit on the timing of UHP metamorphism. These data indicate that most zircons formed during uplift and cooling at P≤15 kbar and do not date UHP conditions directly. Thus, there is no evidence from zircon ages that melts were present during UHP metamorphism (contra Gordon et al., 2013) and possibly facilitated UHP exhumation. Although we agree the occurrence of UHP melts may be consistent with phase equilibria of felsic rocks depending on exact P-T conditions and availability of water (e.g. Huang and Wyllie, 1981; Hermann and Spandler, 2008), crystallization of zircon during melting appears highly unlikely (Figs. 3B, 5;

298 Kelsey et al., 2008; Kelsey and Powell, 2011). Rather, zircons from felsic rocks, including in UHP
299 terranes, more likely date melt crystallization at relatively low P.
300
301 **Papua-New Guinea.** The D'Entrecasteaux Islands in southeastern Papua New Guinea host
302 Earth's youngest HP and UHP rocks (<10 Ma; Baldwin et al., 1993, 2004, 2008; Monteleone et al.,
303 2007; Zirakparvar et al., 2011), and have attracted several chronologic studies to understand how
304 such deep rocks could be transported so quickly to Earth's surface. Here we focus on U-Pb zircon
305 ages (Baldwin et al., 2004; Monteleone et al., 2007; Gordon et al., 2012; Zirakparvar et al., 2014) in
306 the context of hornblende and muscovite $^{40}Ar/^{39}Ar$ cooling ages of 1.5-4 Ma (Baldwin et al., 1993), a
307 zircon age from inclusions in UHP garnet of 7.9±1.9 Ma (Monteleone et al., 2007), and a UHP garnet
308 Lu-Hf age of 7.1±0.7 Ma (Zirakparvar et al., 2011; Fig. 7). Unlike titanite data from the Western
309 Gneiss Region, a high-T temperature-time path is not currently constrained, but given peak
310 metamorphic temperatures of ~700 °C (Monteleone et al., 2007; Baldwin et al., 2008), the Lu-Hf
311 garnet age is likely the most reliable measure of the age of (UHP) garnet growth. Lutetium is
312 homogeneously distributed in these garnets, and X-ray maps indicate that garnets were slightly
313 dissolved but did not experience diffusive uptake on rims that might bias Lu-Hf ages (Zirakparvar et
314 al., 2011).
315 An age probability density plot and a histogram for zircon ages clearly demonstrate
316 chronologically distinct populations (multiple resolvable peaks), with a spread between ~9 to ~2 Ma
317 (Fig. 7). The presumed age of peak HP/UHP metamorphism (c.7-8 Ma from garnet Lu-Hf and zircon
318 inclusions in garnet; Monteleone et al., 2007; Zirakparvar et al., 2011) does overlap 25-30% of zircon
319 ages, but nearly 70% of zircon ages are younger at 2σ statistical significance, and only one age is
320 statistically older. Some zircon ages overlap $^{40}Ar/^{39}Ar$ cooling ages from hornblende and muscovite,
321 again indicating post-peak HP/UHP crystallization, as expected from our models. Although less
322 definitive than for the Western Gneiss Region rocks, these data again support the view that much
323 zircon in eclogites forms after peak P-T conditions.
324 A counterargument to our interpretation focuses on high-precision (±0.2 Ma) CA-TIMS

analyses of individual zircons from eclogite, which have been interpreted to indicate peak-HP/UHP metamorphism between 4.6 and 5.6 Ma (Gordon et al., 2012). We emphasize, however, the relatively large uncertainties in $^{207}Pb/^{235}U$ ratios and ages, the linearity of Concordia, which precludes identification of mixed ages between young (0 to 20 Ma) components for these data, and the prior documentation of multiple, chronologically distinct domains in zircons from the area (Monteleone et al., 2007; Gordon et al., 2012; Fig. 7). These concerns overshadow the precision of the $^{206}Pb/^{238}U$ ages and ultimately introduce chronologic ambiguities of at least ±4 Ma that render the CA-TIMS dates petrogenetically and tectonically untrustworthy. Similar ambiguity in age interpretation was demonstrated for metamorphic monazite in other orogens, for example the Himalaya (Harrison et al., 2002; Kohn et al., 2005) and the New England Appalachians (Pyle and Spear, 2003), and consequently geochronologists now rarely employ whole- or even partial-grain TIMS analysis in this endeavor.

Different elements, different perspectives?

One possible criticism of our analysis focuses on several UHP terranes that contain zircon with coesite or diamond inclusions, for example at Kaghan (Kaneko et al., 2003), Kokchetav (Sobolev et al., 1994), Dabie Shan (Tabata et al., 1998), east Greenland (McClelland et al., 2006), the Western Gneiss Region (Carswell et al., 2003b), and the Alps (Schertl and Schreyer, 1996). If most metamorphic zircon forms relatively late in the metamorphic cycle at low-P, how can such UHP zircon form? In fact, our models do predict growth of UHP zircon (e.g. Alpine-type path, Figs 2-5), and although the amount of zircon produced is small, geochronologists will preferentially seek out and analyze zircons with coesite or diamond inclusions. So perhaps reports of UHP inclusions in zircon overrepresent abundances. Coesite might also be introduced along cracks in older zircons (i.e. pseudoinclusions: Gebauer et al., 1997). Nonetheless, alternative options for producing UHP zircon seem worth exploring. We first discuss chemical-thermodynamic drivers related to mass balance, then mechanisms of grain coarsening and growth independent of chemistry.

Chemically, our mass balance models all assume that in quartz-saturated rocks Zr is the sole

control on zircon stability. But if zircon hosts elements that are shared by other minerals, zircon dissolution and growth might be coupled to reactions among other minerals in ways that our models do not predict. For example, an analogy may be drawn between Ca in plagioclase and garnet in metapelitic bulk compositions: garnet growth necessitates the consumption of plagioclase, specifically its anorthite component, to maintain Ca mass balance (Spear et al, 1990), just as garnet growth theoretically necessitates the consumption of zircon to maintain Zr mass balance with increasing T (Figs. 4-5). However, plagioclase also contains Na, so coupling to other Na-bearing minerals in a rock (e.g. Na-bearing micas) can result in net growth of plagioclase, even as garnet grows. Slow diffusion in plagioclase and zircon implies that reequilibration mechanistically requires dissolution and reprecipitation, and domain- or patchy-zoning in both minerals attest to this reequilibration mechanism. Possibly reactions involving minor or trace elements such as Hf or HREE, rather than Zr alone, affect zircon's stability. Although we acknowledge that the tiny whole-rock free energy changes attending reactions among trace components in minerals may not destabilize zircon, the mass balance calculations are straightforward and illustrate whether such a mechanism is even conceivable.

In principle, Hf mass balance among matrix silicates and zircon might drive zircon recrystallization, at least in metabasalts. A typical MORB basalt contains ~100 ppm Zr and ~2.5 ppm Hf (see Arevalo and McDonough, 2010). If all Zr and Hf were hosted in zircon, zircons would have ~12000 ppm Hf, comparable to, but slightly higher than, the mean for Laurentian zircons from felsic rocks (8000±2000 (1σ) ppm; J. Crowley, unpubl. data). Among metamorphic minerals, hornblende, clinopyroxene and garnet can take several hundred ppb Hf, and titanite can host over 10 ppm (e.g., see Spandler et al., 2003; Lü et al., 2012; Xiao et al., 2013). Although these contents are low, they can account for a significant fraction of the Hf budget. For example:

(3.4 wt% Ttn)(10 ppm Hf) = 0.34 ppm Hf (=10-15% of total Hf)

where the weight fraction of titanite corresponds to our modeled assemblages. Especially during the early stages of metamorphism, when Zr contents of silicates are low (≤1% of total Zr), titanite growth with 10 ppm Hf implies dissolution *and reprecipitation* of zircon. Reprecipitation occurs because the

large flux of Zr cannot be accommodated in matrix minerals, so zircon with a lower Hf content must form. That is, Hf and Zr mass balance could in principle drive a slight reduction in zircon mode to provide Zr to matrix minerals (≤1%), but larger-scale dissolution-reprecipitation of zircon (10-15%) to provide sufficient Hf. A similar prediction can be made using Zr/Hf ratios: the average Zr/Hf weight ratio for zircon is ~60 (J. Crowley, unpubl. data), whereas the ratio in metamorphic minerals averages ~20 (most silicates) to ~40 (garnet; Bea et al., 2006). Thus, matrix mineral growth would require tapping a greater reservoir of zircon for its Hf than for its Zr, which would presumably occur through dissolution-reprecipitation. Recrystallized zircon should exhibit decreased Hf concentrations, however, and little evidence supports this prediction. For example, *in situ* analyses (Whitehouse and Platt, 2003) and depth profiling (Zirakparvar et al., 2014) show both higher and lower Hf concentrations in metamorphic rims compared to inherited cores.

Otherwise, the next most abundant trace elements in zircon are P and HREE. Equilibria involving apatite should buffer P contents in minerals, so we do not believe P mass balance affects zircon stability (also P in zircon is charge balanced to trivalent cations anyway, e.g. $REE^{3+}P^{5+} = Zr^{4+}Si^{4+}$). Metamorphic overgrowths in zircon do show dramatic decreases in HREE and Y because garnet scavenges the same elements (e.g. Schaltegger et al., 1999; Rubatto, 2002; Whitehouse and Platt, 2003). It remains an open question whether these decreases reflect a primary dependence of zircon stability on garnet growth through REE coupling, or whether zircon dissolves and reprecipitates for some other reason(s) and simply reequilibrates with garnet at a lower REE content. Nonetheless, mass balance calculations for HREE again imply major dissolution of zircon, as follows using Yb for illustration. Suppose a basalt contains 3 ppm Yb (Arevalo and McDonough, 2010), which is initially hosted entirely in zircon. If garnet contains 10 ppm Yb and reaches 15% of the mass of the rock, then 50% of zircon would have to dissolve to provide sufficient HREE to garnet. So little zircon is required to supply Zr, however, that most of the dissolved zircon would reprecipitate with a lower HREE content.

Are Hf and HREE likely drivers of zircon dissolution and reprecipitation? As mentioned previously, small free energy changes would seem to disfavor this mechanism. Furthermore,

406 although zircon can form at surprisingly low T (Dempster et al., 2004), metamorphic zircon growth
407 appears suppressed at lower metamorphic grades (Vorhies et al., 2013) where titanite and garnet
408 first nucleate and the calculations above are most relevant. These considerations imply that, to
409 explain recrystallization of zircon during prograde metamorphism, other factors must play a role,
410 such as dissolution of microcrystals or radiation-damaged portions of crystals, with reprecipitation as
411 overgrowths on matrix grains (e.g. Dempster et al., 2008; although see Carlson, 1999, for arguments
412 against Ostwald ripening for crystals larger than ~1 μm). Some studies of metamorphic zircon
413 dissolution-recrystallization additionally implicate reactive fluids, even at temperatures well below
414 melt stability (e.g. ≤500 °C; King et al., 2003; Tomaschek et al., 2003). If such processes operate
415 effectively, a specific zircon crystal might grow as other crystals dissolve, producing prograde zircon
416 overgrowths even at constant or slightly decreasing zircon mode overall. Although presently
417 speculative, the operation of these lower-T prograde processes might be reflected in the progressive
418 loss of smallest grains and growth of coarsest grains, changing crystal size distributions with
419 increasing metamorphic grade.

420 Zircon recrystallization might perhaps produce a distinctive trace element signature, but,
421 more likely, the recycling of elements through different generations of zircon and tapping of
422 previously unreacted zircon could well pose a serious challenge to trace element-based petrogenetic
423 interpretations of zircon and other minerals. For example, garnet growth should deplete the matrix in
424 HREE, and in the context of a fixed trace element reservoir develop a Rayleigh-like zoning pattern
425 (e.g. Lapen et al., 2003; Kohn, 2009). If, however, zircon reactivity changes during metamorphism,
426 the matrix reservoir of HREE is not as large as indicated by whole-rock measurements, so core
427 compositions are lower than expected, and previously unreacted zircon can replenish the matrix
428 reservoir. Such a process might explain differences between measured trace element zoning profiles
429 in garnets vs. Rayleigh distillation model predictions. Although garnets do commonly show “bell-
430 shaped” Y+HREE depletions from core to rim (e.g. Kohn, 2009), they rarely achieve the low
431 concentrations near rims that models predict for a fixed reservoir. This behavior implies some
432 continued source of HREE, perhaps through kinetic limitations to HREE transport through the matrix

(Skora et al., 2006), but possibly from progressively recrystallizing or reacting zircon. Further exploration of zircon crystal sizes and chemistry in petrogenetic context awaits future study.

Implications

Our analysis contradicts the assumption that metamorphic zircon should inevitably record peak pressure conditions, rather, from a mass balance perspective, it should preferentially grow during exhumation and cooling, and rarely record either the transition to eclogite facies or UHP conditions. Although other mechanisms can possibly drive growth of specific zircon crystals (e.g. overall grain coarsening, fluid-mediated dissolution-reprecipitation, etc.), the challenge will be to identify prograde, peak-P or peak-T domains in zircon, as our models predict they will be in the minority. Published petrogenetic and tectonic interpretations should be reevaluated, especially because data from at least two UHP terranes (Western Gneiss Region and Papua New Guinea) imply that most zircon ages indeed postdate UHP metamorphism. Alternative geochemical indicators of "UHP zircon" must be developed, because Eu-anomaly presence/absence and flat HREE patterns are either equivocal or do not discriminate among a large range of P-T conditions. Currently, our best hope of dating UHP metamorphism focuses on *in situ* analysis of zircon domains that actually host UHP inclusions, rather than generic indicators of the eclogite facies, such as garnet or omphacite. Alternatively, Ti-in-zircon thermometry (Watson et al., 2006) might be combined with thermoba-Raman-try of inclusions (Kohn, 2014) to recover P-T conditions independent of geochemical assumptions. Analysts should avoid whole-grain analysis via TIMS, which inevitably mixes chronologically distinct domains formed via different reactions at different times along a rock's P-T path.

Acknowledgments

Funded by NSF grants EAR1048124 and EAR1321897. We thank Suzanne Baldwin and Horst Marschall for their insightful reviews, Thomas Mueller for his expert editorial management, and Jim Crowley for sharing unpublished trace element data for thousands of zircons.

References cited

Arevalo, R. Jr., and McDonough, W.F. (2010) Chemical variations and regional diversity observed in MORB. Chemical Geology, 271, 70-85.

Baldwin, S.L., Lister, G.S., Hill, E.J., Foster, D.A., and McDougall, I. (1993) Thermochronologic constraints on the tectonic evolution of active metamorphic core complexes, D'Entrecasteaux Islands, Papua New Guinea. Tectonics, 12, 611-628.

Baldwin, S.L., Monteleone, B.D., Webb, L.E., Fitzgerald, P.G., Grove, M., and Hill, E.J. (2004) Pliocene eclogite exhumation at plate tectonic rates in eastern Papua New Guinea. Nature, 431, 263-267.

Baldwin, S.L., Webb, L.E., and Monteleone, B.D. (2008) Late Miocene coesite-eclogite exhumed in the Woodlark Rift. Geology, 36, 735-738.

Bea, F., Montero, P., and Ortega, M. (2006) A LA-ICP-MS evaluation of Zr reservoirs in common crustal rocks: implications for Zr and Hf geochemistry, and zircon-forming processes. The Canadian Mineralogist, 44, 693-714.

Beckman, V., Möller, C., Söderlund, U., Corfu, F., Pallon, J., and Chamberlain, K.R. (2014) Metamorphic zircon formation at the transition from gabbro to eclogite in Trollheimen-Surnadalen, Norwegian Caledonides. Geological Society, London, Special Publications, 390, 403-424.

Berman, R.G. (1988) Internally-consistent thermodynamic data for minerals in the system Na_2O-K_2O-CaO-MgO-FeO-Fe_2O_3-Al_2O_3- SiO_2-TiO_2-H_2O-CO_2. Journal of Petrology, 29, 445-522.

Berman, R.G., and Aranovich, L.Y. (1996) Optimized standard state and solution properties of minerals 1. Model calibration for olivine, orthopyroxene, cordierite, garnet, and ilmenite in the system FeO-MgO-CaO-Al_2O_3-TiO_2-SiO_2. Contributions to Mineralogy and Petrology, 126, 1-24.

Bingen, B., Austrheim, H., and Whitehouse, M. (2001) Ilmenite as a source for zirconium during high-grade metamorphism? Textural evidence from the Caledonides of western Norway and implications for zircon geochronology. Journal of Petrology, 42, 355-375.

Bloch, E. (2013) Diffusion kinetics of lutetium and hafnium in garnet and clinopyroxene:

Experimental determination and consequences for 176Lu-176Hf geochronometry. Department of Geosciences, p. 197. University of Arizona, Tucson.

Burton, K.W., Kohn, M.J., Cohen, A.S., and O'Nions, R.K. (1995) The relative diffusion of Pb, Nd, Sr and O in garnet. Earth and Planetary Science Letters, 133, 199-211.

Carlson, W.D. (1999) The case against Ostwald ripening of porphyroblasts. The Canadian Mineralogist, 37(2), 403-413.

Carswell, D.A., Brueckner, H.K., Cuthbert, S.J., Mehta, K., and O'Brien, P.J. (2003a) The timing of stabilisation and the exhumation rate for ultra-high pressure rocks in the Western Gneiss Region of Norway. Journal of Metamorphic Geology, 21(6), 601-612.

Carswell, D.A., Tucker, R.D., O'Brien, P.J., and Krogh, T.E. (2003b) Coesite micro-inclusions and the U/Pb age of zircons from the Hareidland Eclogite in the Western Gneiss Region of Norway. Lithos, 67, 181-190.

Chambers, J.A., and Kohn, M.J. (2012) Titanium in muscovite, biotite, and hornblende: Modeling, thermometry and rutile activities in metapelites and amphibolites. American Mineralogist, 97, 543-555.

Chen, Y.-X., Zheng, Y.-F., and Hu, Z. (2013) Petrological and zircon evidence for anatexis of UHP quartzite during continental collision in the Sulu orogen. Journal of Metamorphic Geology, 31, 389-413.

Cherniak, D.J. (2010) Diffusion in accessory minerals: zircon, titanite, apatite, monazite and xenotime. Reviews in Mineralogy and Geochemistry, 72, 827-869.

Chernoff, C.B., and Carlson, W.D. (1999) Trace element zoning as a record of chemical disequilibrium during garnet growth. Geology, 27(6), 555-558.

Chopin, C., Henry, C., and Michard, A. (1991) Geology and petrology of the coesite-bearing terrain, Dora-Maira Massif, western Alps. European Journal of Mineralogy, 3, 263-291.

de Capitani, C., and Petrakakis, I. (2010) The computation of equilibrium assemblage diagrams with Theriak/Domino software. American Mineralogist, 95, 1006-1016.

Degeling, H., Eggins, S., and Ellis, D.J. (2001) Zr budgets for metamorphic reactions, and the

formation of zircon from garnet breakdown. Mineralogical Magazine, 65, 749-758.

Dempster, T.J., Hay, D.C., and Bluck, B.J. (2004) Zircon growth in slate. Geology, 32, 221-224.

Dempster, T.J., Hay, D.C., Gordon, S.H., and Kelly, N.M. (2008) Micro-zircon: origin and evolution during metamorphism. Journal of Metamorphic Geology, 26, 499-507.

England, P.C., and Thompson, A.B. (1984) Pressure - temperature - time paths of regional metamorphism, Part I: Heat transfer during the evolution of regions of thickened continental crust. Journal of Petrology, 25, 894-928.

Fraser, G., Ellis, D., and Eggins, S. (1997) Zirconium abundance in granulite-facies minerals, with implications for zircon geochronology in high-grade rocks. Geology, 25, 607-610.

Frei, D., Liebscher, A., Franz, G., and Dulski, P. (2004) Trace element geochemistry of epidote minerals. Reviews in Mineralogy and Geochemistry, 56, 553-605.

Ganguly, J., Tirone, M., and Hervig, R.L. (1998) Diffusion kinetics of samarium and neodymium in garnet, and a method for determining cooling rates of rocks. Science, 281, 805-807.

Gao, X.-Y., Zheng, Y.-F., Chen, Y.-X., and Guo, J. (2012) Geochemical and U-Pb age constraints on the occurrence of polygenetic titanites in UHP metagranite in the Dabie orogen. Lithos, 136-139, 93-108.

Gebauer, D., Schertl, H.P., Brix, M., and Schreyer, W. (1997) 35 Ma old ultrahigh-pressure metamorphism and evidence for very rapid exhumation in the Dora Maira Massif, Western Alps. Lithos, 41, 5-24.

Gordon, S.M., Little, T.A., Hacker, B.R., Bowring, S.A., Korchinski, M., Baldwin, S.L., and Kylander-Clark, A.R.C. (2012) Multi-stage exhumation of young UHP-HP rocks: Timescales of melt crystallization in the D'Entrecasteaux Islands, southeastern Papua New Guinea. Earth and Planetary Science Letters, 351-352, 237-246.

Gordon, S.M., Whitney, D.L., Teyssier, C., and Fossen, H. (2013) U-Pb dates and trace-element geochemistry of zircon from migmatite, Western Gneiss Region, Norway: Significance for history of partial melting in continental subduction. Lithos, 170-171, 35-53.

Griffin, W.L., and Brueckner, H.K. (1980) Caledonian Sm-Nd ages and a crustal origin for Norwegian

eclogites. Nature, 285, 319-321.

Harrison, T.M., Catlos, E.J., and Montel, J.M. (2002) U-Th-Pb dating of phosphate minerals. In M.J. Kohn, J. Rakovan, and J.M. Hughes, Eds. Phosphates: Geochemical, Geobiological, and Materials Importance, 48, p. 523-558.

Henry, D.J., Guidotti, C.V., and Thomson, J.A. (2005) The Ti-saturation surface for low-to-medium pressure metapelitic biotites: Implications for geothermometry and Ti-substitution mechanisms. American Mineralogist, 90, 316-328.

Hermann, J., and Spandler, C.J. (2008) Sediment melts at sub-arc depths: an experimental study. Journal of Petrology, 49(4), 717-740.

Hermann, J., Rubatto, D., Korsakov, A., and Shatsky, V.S. (2001) Multiple zircon growth during fast exhumation of diamondiferous, deeply subducted continental crust (Kokchetav Massif, Kazakhstan). Contributions to Mineralogy and Petrology, 141, 66-82.

Hokada, T., and Harley, S.L. (2004) Zircon growth in UHT leucosome: constraints from zircon-garnet rare earth elements (REE) relations in Napier Complex, East Antarctica. Journal of Mineralogical and Petrological Sciences, 99, 180-190.

Holland, T.J.B., and Powell, R. (1998) An internally consistent thermodynamic data set for phases of petrological interest. Journal of Metamorphic Geology, 16(3), 309-343.

Huang, W.L., and Wyllie, P.J. (1981) Phase relationships of S-type granite with H_2O to 35 kbar. Muscovite granite from Harney Peak, South Dakota. Journal of Geophysical Research, 86, 10515-10529.

Jamtveit, B., Carswell, D.A., and Mearns, E.W. (1991) Chronology of the high-pressure metamorphism of Norwegian garnet perdotites/pyroxenites. Journal of Metamorphic Geology, 9, 125-139.

Jiao, S., Guo, J., Harley, S.L., and Peng, P. (2013) Geochronology and trace element geochemistry of zircon, monazite and garnet from the garnetite and/or associated other high-grade rocks: Implications for Palaeoproterozoic tectonothermal evolution of the Khondalite Belt, North China Craton. Precambrian Research, 237, 78-100.

568 Kaneko, Y., Katayama, I., Yamamoto, H., Misawa, K., Ishikawa, M., Rehman, H.U., Kausar, A.B.,
569 and Shiraishi, K. (2003) Timing of Himalayan ultrahigh-pressure metamorphism: sinking rate and
570 subduction angle of the Indian continental crust beneath Asia. Journal of Metamorphic Geology,
571 21(6), 589-599.
572 Kelsey, D.E., and Powell, R. (2011) Progress in linking accessory mineral growth and breakdown to
573 major mineral evolution in metamorphic rocks: a thermodynamic approach in the Na_2O-CaO-
574 K_2O-FeO-MgO-Al_2O_3-SiO_2-H_2O-TiO_2-ZrO_2 system. Journal of Metamorphic Geology, 29, 151-
575 166.
576 Kelsey, D.E., Clark, C., and Hand, M. (2008) Thermobarometric modelling of zircon and monazite
577 growth in melt-bearing systems: examples using model metapelitic and metapsammitic
578 granulites. Journal of Metamorphic Geology, 26, 199-212.
579 King, R.L., Kohn, M.J., and Eiler, J.M. (2003) Constraints on the petrologic structure of the
580 subduction zone slab-mantle interface from Franciscan Complex exotic ultramafic blocks.
581 Geological Society of America Bulletin, 115, 1097-1109.
582 Kohn, M.J. (2004) Oscillatory- and sector-zoned garnets record cyclic (?) rapid thrusting in central
583 Nepal. Geochemistry Geophysics Geosystems, 5, 10.1029/2004gc000737.
584 Kohn, M.J. (2009) Models of garnet differential geochronology. Geochimica et Cosmochimica Acta,
585 73, 170-182.
586 Kohn, M.J. (2014) "Thermoba-Raman-try": Calibration of spectroscopic barometers and
587 thermometers for mineral inclusions. Earth and Planetary Science Letters, 388, 187-196.
588 Kohn, M.J., and Corrie, S.L. (2011) Preserved Zr-temperatures and U-Pb ages in high-grade
589 metamorphic titanite: evidence for a static hot channel in the Himalayan orogen. Earth and
590 Planetary Science Letters, 311, 136-143.
591 Kohn, M.J., and Spear, F.S. (2015) Metamorphic chronology comes of age: past achievements and
592 future prospects. American Mineralogist, in review.
593 Kohn, M.J., Wieland, M.S., Parkinson, C.D., and Upreti, B.N. (2005) Five generations of monazite in
594 Langtang gneisses: implications for chronology of the Himalayan metamorphic core. Journal of

595 Metamorphic Geology, 23(5), 399-406.
596 Krogh, T.E., Kamo, S.L., Robinson, P., Terry, M.P., and Kwok, K. (2011) U-Pb zircon geochronology
597 of eclogites from the Scandian Orogen, northern Western Gneiss Region, Norway: 14-20 million
598 years between eclogite crystallization and return to amphibolite-facies conditions. Canadian
599 Journal of Earth Science, 48, 441-472.
600 Kylander-Clark, A.R.C., Hacker, B.R., Johnson, C.M., Beard, B.L., Mahlen, N.J., and Lapen, T.J.
601 (2007) Coupled Lu-Hf and Sm-Nd geochronology constrains prograde and exhumation histories
602 of high- and ultrahigh-pressure eclogites from western Norway. Chemical Geology, 242, 137-
603 154.
604 Kylander-Clark, A.R.C., Hacker, B.R., Johnson, C.M., Beard, B.L., and Mahlen, N.J. (2009) Slow
605 subduction of a thick ultrahigh-pressure terrane. Tectonics, 28, doi:10.1029/2007TC002251.
606 Lapen, T.J., Johnson, C.M., Baumgartner, L.P., Mahlen, N.J., Beard, B.L., and Amato, J.M. (2003)
607 Burial rates during prograde metamorphism of an ultra-high-pressure terrane: an example from
608 Lago di Cignana, western Alps, Italy. Earth and Planetary Science Letters, 215, 57-72.
609 Liebscher, A., Franz, G., Frei, D., and Dulski, P. (2007) High-pressure melting of eclogite and the P-
610 T-X history of tonalitic to trondhjemitic zoisite-pegmatites, Münchberg Massif, Germany. Journal
611 of Petrology, 48, 1001-1019.
612 Lü, Z., Zhang, L., Du, J., Yang, X., Tian, Z., and Xia, B. (2012) Petrology of HP metamorphic veins in
613 coesite-bearing eclogite from western Tianshan, China: Fluid processes and elemental mobility
614 during exhumation in a cold subduction zone. Lithos, 136-139, 168-186.
615 McClelland, W.C., Power, S.E., Gilotti, J.A., Mazdab, F.K., and Wopenka, B. (2006) U-Pb SHRIMP
616 geochronology and trace element geochemistry of coesite-bearing zircons, North-East
617 Greenland Caledonides. Geological Society of America Special Paper, 403, 23-43.
618 Monteleone, B.D., Baldwin, S.L., Webb, L.E., Fitzgerald, P.G., Grove, M., and Schmitt, A.K. (2007)
619 Late Miocene-Pliocene eclogite facies metamorphism, D'Entrecasteaux Islands, SE Papua New
620 Guinea. Journal of Metamorphic Geology, 25, 245-265.
621 Mørk, M.B.E., and Mearns, E.W. (1986) Sm-Nd isotopic systematics of a gabbro-eclogite transition.

Lithos, 19, 255-267.

Orejana, D., Villaseca, C., Armstrong, R.A., and Jeffries, T.E. (2011) Geochronology and trace element chemistry of zircon and garnet from granulite xenoliths: constraints on the tectonothermal evolution of the lower crust under central Spain. Lithos, 124, 103-116.

Pyle, J.M., and Spear, F.S. (2003) Four generations of accessory-phase growth in low-pressure migmatites from SW New Hampshire. American Mineralogist, 88, 338-351.

Root, D.B., Hacker, B.R., Mattinson, J.M., and Wooden, J.L. (2004) Zircon geochronology and ca. 400 Ma exhumation of Norwegian ultrahigh-pressure rocks: an ion microprobe and chemical abrasion study. Earth and Planetary Science Letters, 228, 325-341.

Rubatto, D. (2002) Zircon trace element geochemistry: partitioning with garnet and link between U-Pb ages and metamorphism. Chemical Geology, 184, 123-138.

Rubatto, D., Hermann, J., and Buick, I.S. (2006) Temperature and bulk composition control on the growth of monazite and zircon during low-pressure anatexis (Mount Stafford, Central Australia). Journal of Petrology, 47, 1973-1996.

Sassi, R., Harte, B., Carswell, D.A., and Yujing, H. (2000) Trace element distribution in Central Dabie eclogites. Contributions to Mineralogy and Petrology, 139, 298-315.

Schaltegger, U., Fanning, C.M., Günther, D., Maurin, J.-C., Schulmann, K., and Gebauer, D. (1999) Growth, annealing and recrystallization of zircon and preservation of monazite in high-grade metamorphism: conventional and in-situ U-Pb isotope, cathodoluminescence and microchemical evidence. Contributions to Mineralogy and Petrology, 134, 186-201.

Schertl, H.-P., and Schreyer, W. (1996) Mineral inclusions in heavy minerals of the ultra-high pressure metamorphic rocks of the Dora Maira Massif and their bearing on the relative timing of the petrological events. Geophyscical Monographs, 95, 331-342.

Schertl, H.P., Schreyer, W., and Chopin, C. (1991) The pyrope-coesite rocks and their country rocks at Parigi, Dora Maira Massif, western Alps - detailed petrography, mineral chemistry and P-T path. Contributions to Mineralogy and Petrology, 108, 1-21.

Skora, S., Baumgartner, L.P., Mahlen, N.J., Johnson, C.M., Pilet, S., and Hellebrand, E. (2006)

649 Diffusion-limited REE uptake by eclogite garnets and its consequences for Lu-Hf and Sm-Nd
650 geochronology. Contributions to Mineralogy and Petrology, 152, 703-720.
651 Sobolev, N.V., Shatsky, V.S., Vavilov, M.A., and Goryanov, S.V. (1994) Zircon from ultrahigh-
652 pressure metamorphic rocks of folded regions as a unique container of inclusions of diamond,
653 coesite and coexisting minerals. Doklady Akademii Nauk, 334, 482-488.
654 Spandler, C., Hermann, J., Arculus, R., and Mavrogenes, J. (2003) Redistribution of trace elements
655 during prograde metamorphism from lawsonite blueschist to eclogite facies; implications for deep
656 subduction-zone processes. Contributions to Mineralogy and Petrology, 146, 205-222.
657 Spear, F.S., Kohn, M.J., Florence, F., and Menard, T. (1990) A model for garnet and plagioclase
658 growth in pelitic schists: Implications for thermobarometry and P-T path determinations. Journal
659 of Metamorphic Geology, 8, 683-696.
660 Spencer, K.J., Hacker, B.R., Kylander-Clark, A.R.C., Andersen, T.B., Cottle, J.M., Stearns, M.A.,
661 Poletti, J.E., and Seward, G.G.E. (2013) Campaign-style titanite U-Pb dating by laser-ablation
662 ICP: Implications for crustal flow, phase transformations and titanite closure. Chemical Geology,
663 341, 84-101.
664 Tabata, H., Yamauchi, K., Maruyama, S., and Liou, J.G. (1998) Tracing the extent of an ultrahigh
665 pressure metamorphic terrane: A mineral inclusion study of zircons and gneisses from the Dabie
666 Mountains. In B. Hacker, and J.G. Liou, Eds. When continents collide: Geodynamics and
667 geochemistry of ultrahigh-pressure rocks, p. 261-274. Kluwer, Dordrecht, Netherlands.
668 Terry, M.P., Robinson, P., Hamilton, M.A., and Jercinovic, M.J. (2000) Monazite geochronology of
669 UHP and HP metamorphism, deformation, and exhumation, Nordøyane, Western Gneiss
670 Region, Norway. American Mineralogist, 85, 1651-1664.
671 Tomaschek, F., Kennedy, A.K., Villa, I.M., Lagos, M., and Ballhaus, C. (2003) Zircons from Syros,
672 Cyclades, Greece – recrystallization and mobilization of zircon during high-pressure
673 metamorphism. Journal of Petrology, 44, 1977-2002.
674 Tomkins, H.S. (2006) Zr-almandine thermodynamics, and implications for zircon equilibria.
675 Geochimica et Cosmochimica Acta, 70, A653.

Vorhies, S.H., Ague, J.J., and Schmitt, A.K. (2013) Zircon growth and recrystallization during progressive metamorphism, Barrovian zones, Scotland. American Mineralogist, 98, 219-230.

Watson, E.B., Wark, D.A., and Thomas, J.B. (2006) Crystallization thermometers for zircon and rutile. Contributions to Mineralogy and Petrology, 151, 413-433.

Whitehouse, M.J., and Platt, J.P. (2003) Dating high-grade metamorphism – constraints from rare-earth elements in zircon and garnet. Contributions to Mineralogy and Petrology, 145, 61-74.

Xiao, Y., Niu, Y., Song, S., Davidson, J., and Liu, X. (2013) Elemental responses to subduction-zone metamorphism: constraints from the North Qilian Mountain, NW China. Lithos, 160-161, 55-67.

Yang, P., and Rivers, T. (2000) Trace element partitioning between coexisting biotite and muscovite from metamorphic rocks, western Labrador; structural, compositional and thermal controls. Geochimica et Cosmochimica Acta, 64(8), 1451-1472.

Young, D.J., Hacker, B.R., Andersen, T.B., and Corfu, F. (2007) Prograde amphibolite facies to ultrahigh-pressure transition along Nordfjord, western Norway: Implications for exhumation tectonics. Tectonics, 26, doi:10.1029/2004TC001781.

Zack, T., Foley, S.F., and Rivers, T. (2002) Equilibrium and disequilibrium trace element partitioning in hydrous eclogites (Trescolmen, Central Alps). Journal of Petrology, 43, 1947-1974.

Zack, T., Moraes, R., and Kronz, A. (2004) Temperature dependence of Zr in rutile: empirical calibration of a rutile thermometer. Contributions to Mineralogy and Petrology, 148, 471-488.

Zirakparvar, N.A., Baldwin, S.L., and Vervoort, J.D. (2011) Lu-HF garnet geochronology applied to plate boundary zones: Insights from the (U)HP terrane exhumed within the Woodlark Rift. Earth and Planetary Science Letters, 309, 56-66.

Zirakparvar, N.A., Baldwin, S.L., and Schmitt, A.K. (2014) Zircon growth in (U)HP quartzo-feldspathic host gneisses exhumed in the Woodlark Rift of Papua New Guinea. Geochemistry, Geophysics, Geosystems, 15, 1258-1282.

Table 1. Zirconium concentrations (ppm) of metamorphic minerals

Mineral	n	Median Zr	Ave Zr (±1s.e.)	Max Zr	Min Zr
Actinolite	8	0.49	0.52±0.13	1.02	0.06
Biotite	67	0.15	0.26±0.02	0.74	0.00
Chlorite	7	0.13	0.13±0.04	0.34	0.02
Clinopyroxene	47	2.20	2.65±0.50	22.92	0.06
Clinozoisite	16	3.52	5.04±1.11	14.50	0.76
Epidote	26	5.65	6.88±0.83	20.60	0.41
Glaucophane	9	0.46	4.97±3.19	27.73	0.06
Ilmenite	10	3.39	3.85±1.05	7.90	0.44
Kyanite	1	0.75			
Lawsonite	5	0.37	0.39±0.09	0.56	0.08
Muscovite/Phengite	48	0.24	0.49±0.08	2.06	0.04
Orthopyroxene	5	0.10	0.37±0.26	1.40	0.00
Plagioclase	35	0.09	0.18±0.04	1.13	0.00
Talc	5	0.14	0.14±0.04	0.25	0.01

Note: n = the number of analyses reported. See supplemental file for garnet and hornblende. Sources: Sassi et al. (2000), Yang and Rivers (2000), Zack et al. (2002), Spandler et al. (2003), Frei et al. (2004), Hokada and Harley (2004), Bea et al. (2006), Rubatto et al. (2006), Liebscher et al. (2007), Orejana et al. (2011), Lü et al. (2012), Chen et al. (2013), Jiao et al. (2013), Xiao et al. (2013), this study.

Figure Captions

Figure 1. Concentration of Zr in garnet and hornblende vs. reciprocal temperature illustrating general negative correlation (i.e., Zr contents increase with increasing T).

Figure 2. Pressure vs. temperature plot of pseudosections, assumed P-T paths, and boundaries on selected mineral stability fields. P-T paths broadly correspond to UHP evolution in the Alps ("Alpine", blue), HT-HP evolution in the Western Gneiss Region ("WGR", purple), and moderate-T – moderate-P evolution predicted by thermal models of continent-continent collision ("CC", green). Dots on paths are points where Zr mass balance was evaluated and plotted in Fig. 3. Mineral abbreviations are Rt = rutile, Pl = plagioclase, Hbl = hornblende, and Grt = garnet. (A) Model using the Berman (1988) thermodynamic database. (B) Model using the Holland and Powell (1998) thermodynamic database.

Figure 3. Simplified P-T plot from Fig. 2A and S2 with isopleths of Zr-in-rutile (Watson et al., 2006). A) MORB compositions. B) Pelitic composition. Tic marks with percentages perpendicular to paths quantify the percent zircon consumed along each path. "Alpine", "WGR", and "CC" refer to typical paths for the Alps, Western Gneiss Region, and thermal model predictions of continent-continent collisions, respectively. At high-T, low-P conditions, isopleths of percent zircon dissolved would roughly parallel Zr-in-rutile isopleths (see also Kelsey and Powell, 2011).

Figure 4. Models of Zr distribution among key phases in the MORB composition. Lines and labels that are darker vs. lighter correspond to thermodynamic models using the Berman (1988) vs. Holland and Powell (1998) thermodynamic databases. In general, zircon dissolves during prograde metamorphism and initial exhumation until either the maximum temperature is reached, or other Ti-bearing minerals form. (A+B) Western Gneiss Region – type model. (C+D) Alpine – type model. (E+F) Continent-continent collisional – type model. Note vertical scale shift for WGR vs. other models. Pl = plagioclase; Rt = rutile; Ttn=titanite; Ilm = ilmenite; Hbl = hornblende; Grt = garnet

Figure 5. Models of Zr distribution among key phases for a metapelitic composition, thermodynamic

database of Holland and Powell (1998). In general, zircon dissolves during prograde metamorphism and initial exhumation until the maximum temperature is reached or melts crystallize. (A+B) Western Gneiss Region – type model. (C+D) Alpine – type model. (E+F) Continent-continent collisional – type model. MORB models (light lines) shown for reference. Note vertical scale shifts compared to Fig. 4 and between 5B (WGR) and 5D, F (Alpine, CC). Pl = plagioclase; Rt = rutile; Ttn=titanite; Ilm = ilmenite; Gln = glaucophane; Grt = garnet

Figure 6. Chronologic data from the Western Gneiss Region HP/UHP terranes. T-t curve (solid black line) is based on titanite data from Spencer et al. (2013), which encode both age and temperature. Dashed line shows possible extension of T-t curve based on likely P-T-t evolution. Titanite is not stable above ~15 kbar. Zircon U-Pb ages (Carswell et al., 2003b; Root et al., 2004; Young et al., 2007; Krogh et al., 2011; Gordon et al., 2013; Beckman et al., 2014) are plotted along inferred T-t curve (slightly offset for visibility at high-T), and dominantly (75%) overlap titanite ages, implying most zircon formed below ~15 kbar, as predicted (Fig. 2). Probability density plot of zircon ages also shows large overlap with titanite ages. A Th-Pb age for monazite inclusion in garnet (Terry et al., 2000), and regional garnet Sm-Nd and Lu-Hf ages (Griffin and Brueckner, 1980; Mørk and Mearns, 1986; Jamtveit et al., 1991; Carswell et al., 2003a; Kylander-Clark et al., 2007, 2009) shown for reference. Zircon, garnet, and monazite ages do not have independent temperature significance. Four titanite analyses exhibit inheritance or bimodality of ages and/or temperature, and are excluded from the overall T-t path.

Figure 7. Age probability density plot for zircon U-Pb ages collected *in situ* via ion microprobe and LA-ICP-MS (Baldwin et al., 2004; Monteleone et al., 2007; Gordon et al., 2012; Zirakparvar et al., 2014). Most (~70%) of ages are statistically younger than the presumed peak UHP metamorphic age (7.1±0.7 Ma, Lu-Hf UHP garnet; 7.9±1.9 Ma, U-Pb zircon inclusion in UHP garnet). Hornblende and muscovite $^{40}Ar/^{39}Ar$ ages (Baldwin et al., 1993) and two TIMS U-Pb zircon ages (Gordon et al., 2012) shown for reference.

759 Fig. S1. Complete pseudosections for MORB.

760 Fig. S2. Pseudosection for pelitic composition.

761

Fig. 1, Kohn et al.

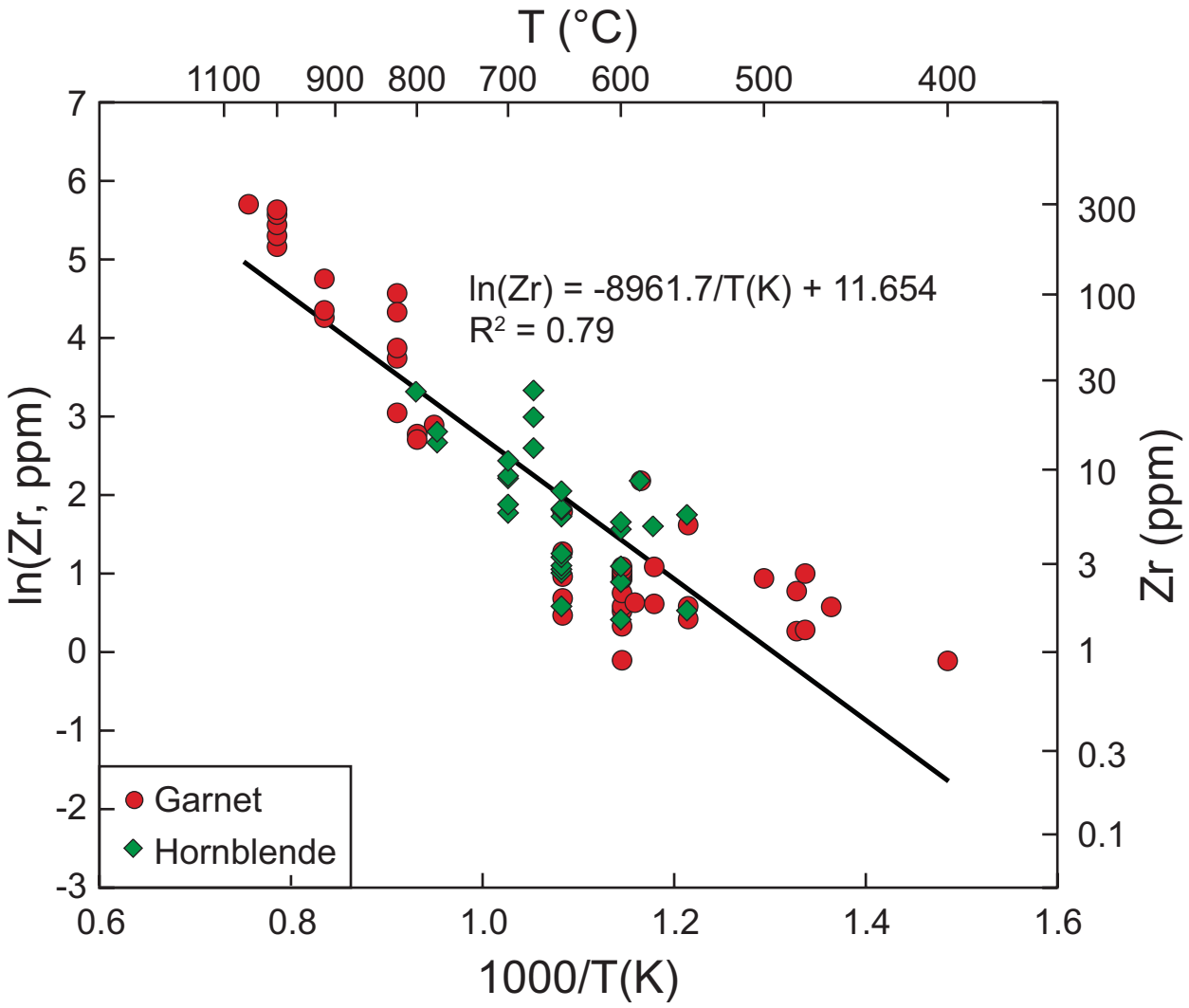

Fig. 2, Kohn et al.

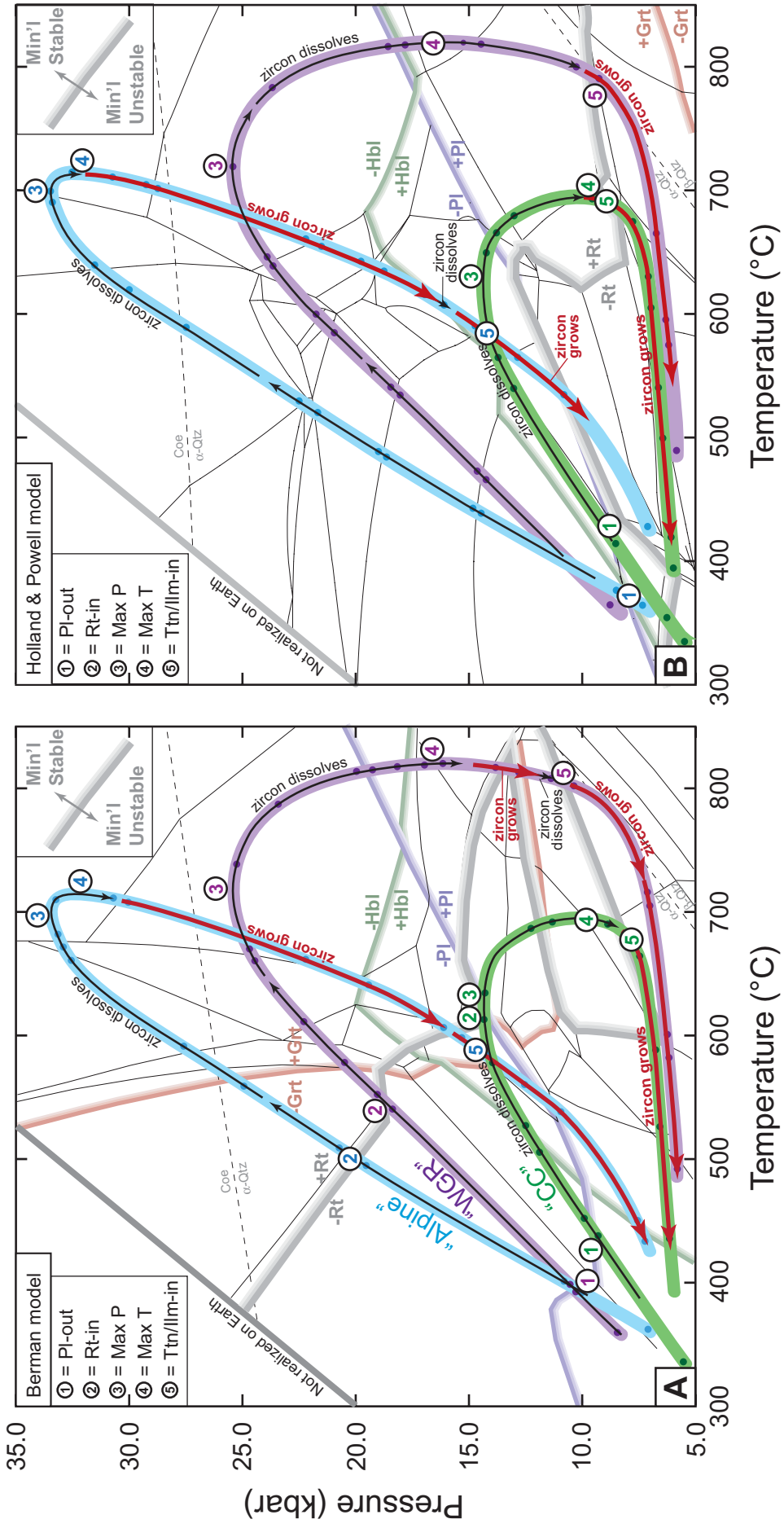

Fig. 3, Kohn et al.

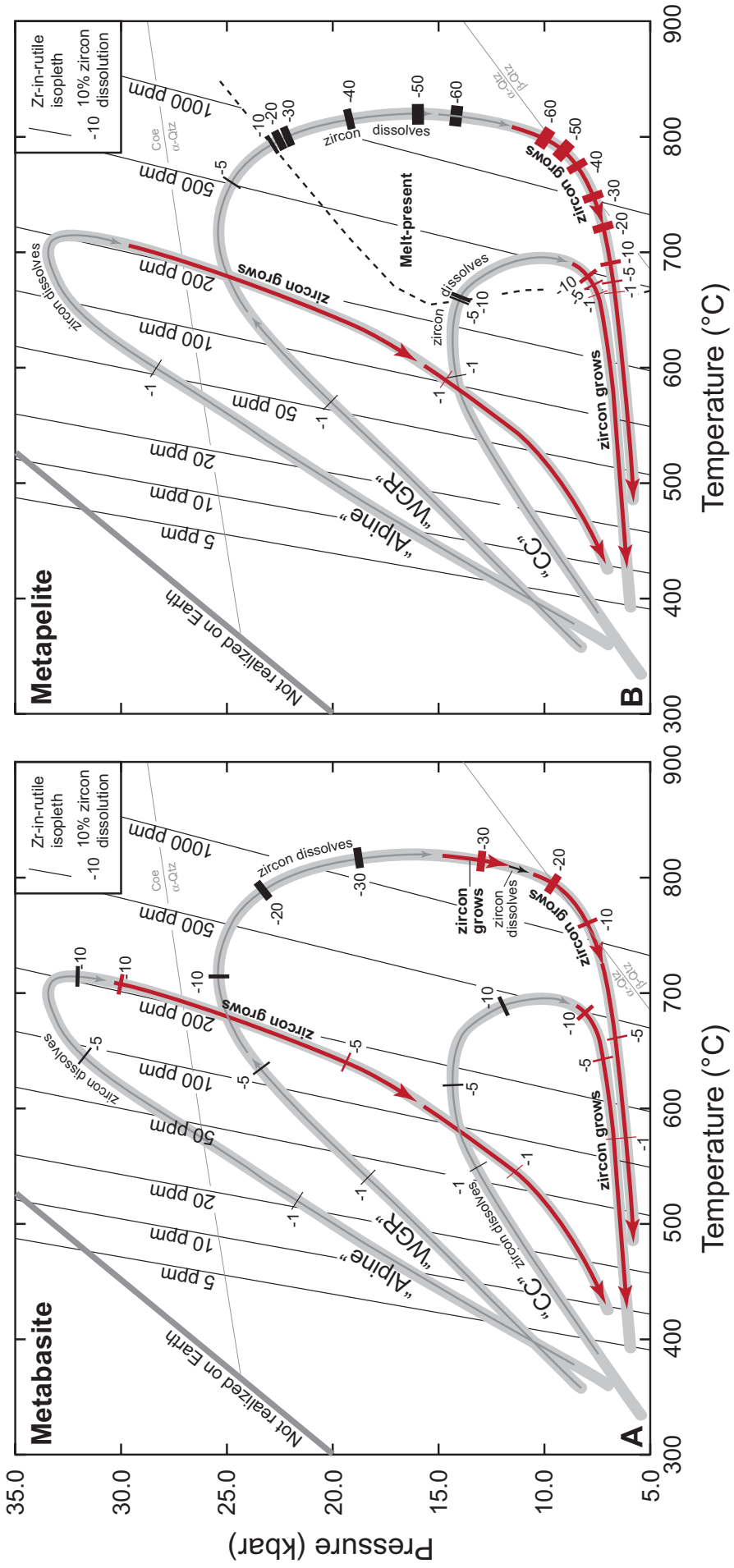

This is a preprint, the final version is subject to change, of the American Mineralogist (MSA)
Cite as Authors (Year) Title. American Mineralogist, in press.
(DOI will not work until issue is live.) DOI: http://dx.doi.org/10.2138/am-2015-5064

Fig. 4, Kohn et al.

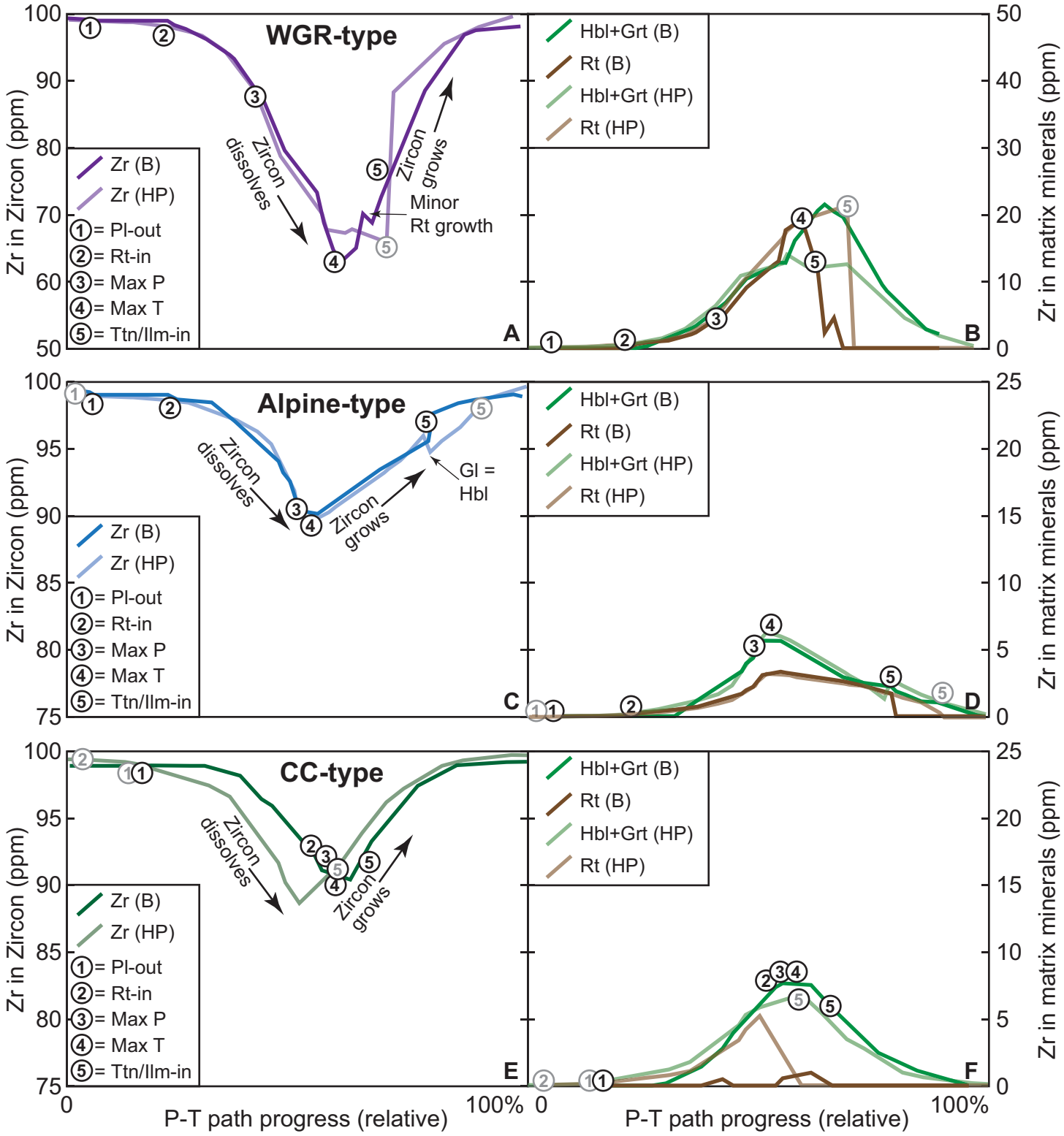

This is a preprint, the final version is subject to change, of the American Mineralogist (MSA)
Cite as Authors (Year) Title. American Mineralogist, in press.
(DOI will not work until issue is live.) DOI: http://dx.doi.org/10.2138/am-2015-5064

Fig. 5, Kohn et al.

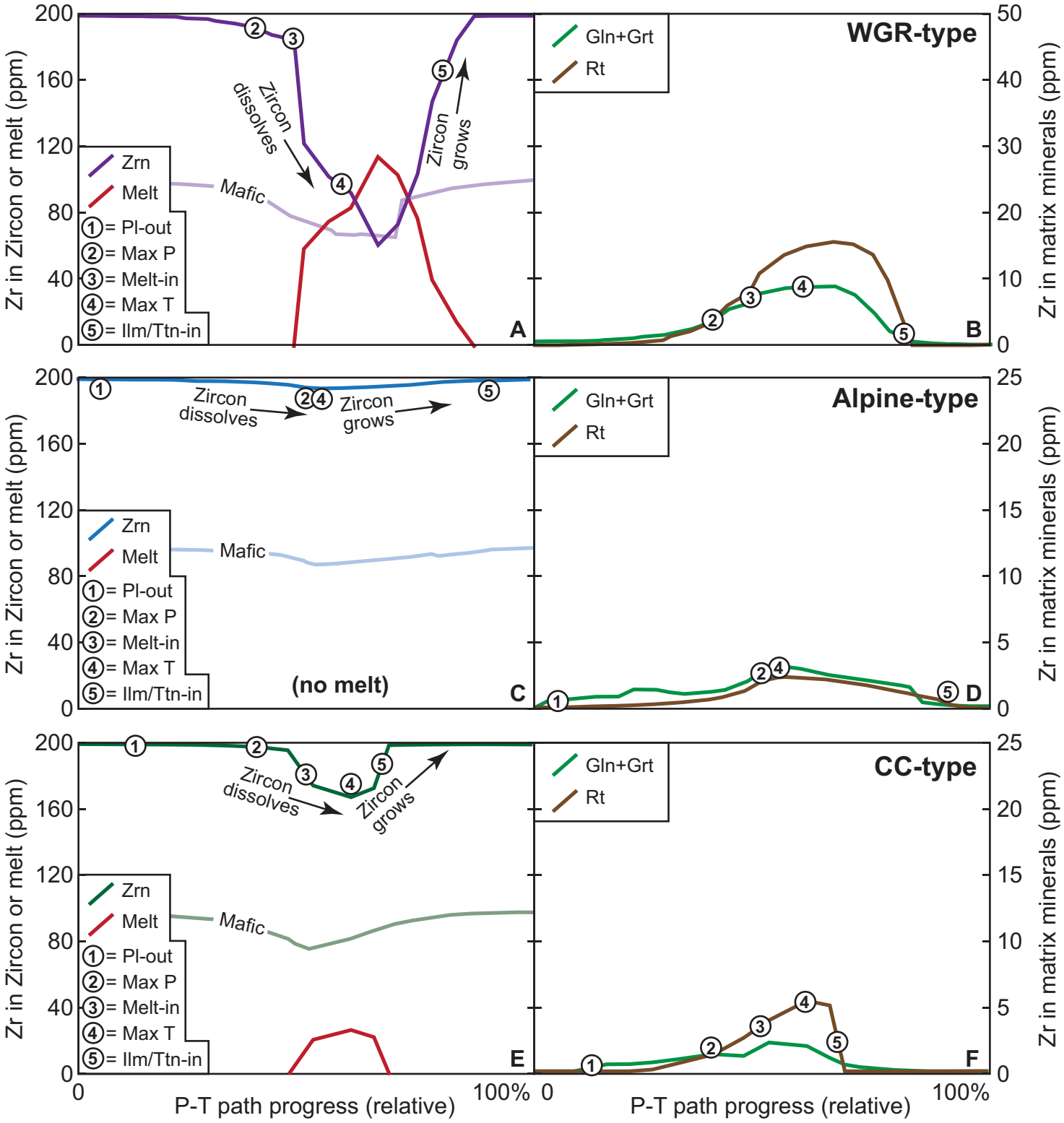

Fig. 6, Kohn et al.

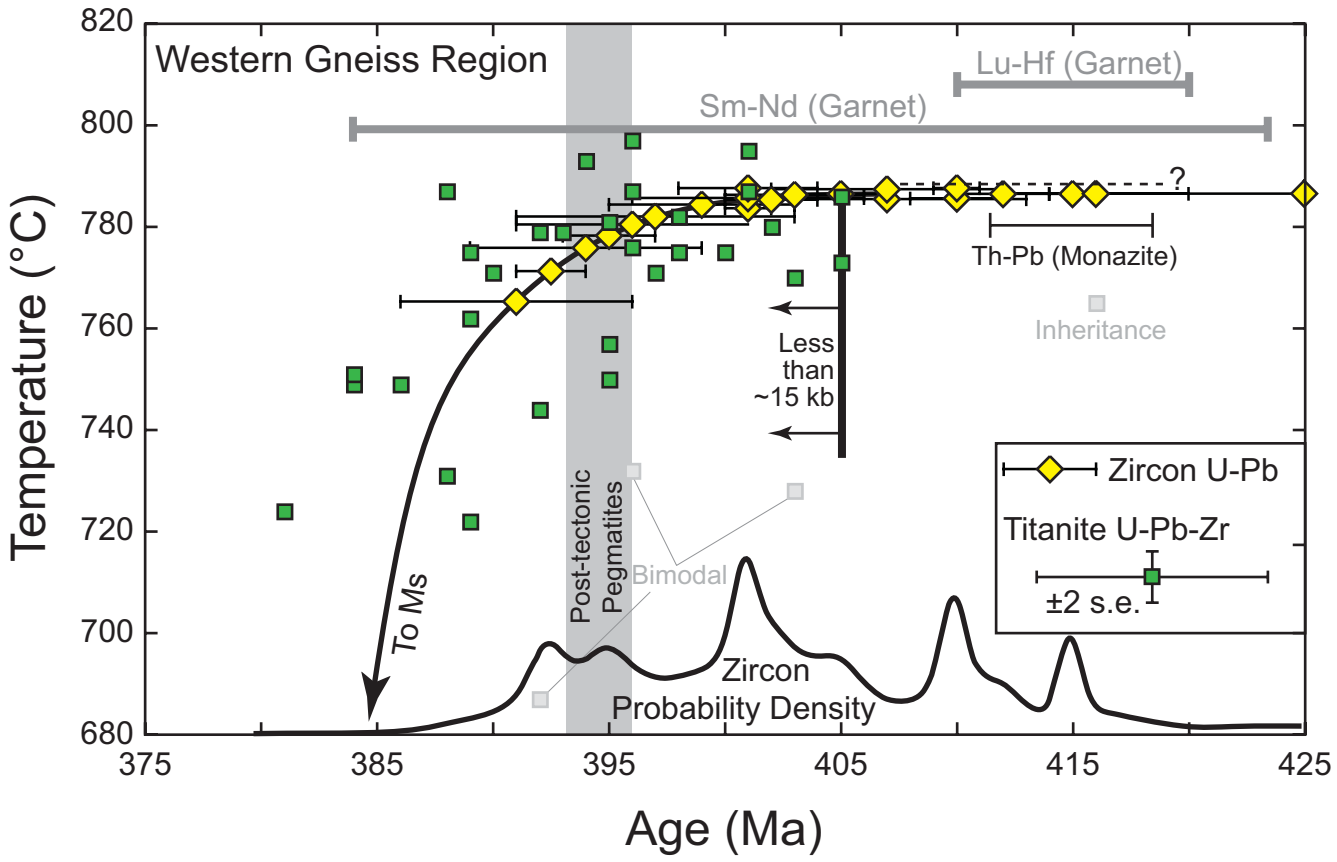

Fig. 7, Kohn et al.